

Cerium Doped Zirconium Dioxide, a Visible-Light Sensitive Photoactive Material of Third Generation

**Chiara Gionco¹, Maria Cristina Paganini¹, Elio Giamello^{1*}, Robertson Burgess²,
Cristiana Di Valentin², Gianfranco Pacchioni².**

¹ Dipartimento di Chimica, Università di Torino and NIS, Nanostructured Interfaces and Surfaces,
Via P. Giuria 7, 10125 Torino, Italy

² Dipartimento di Scienza dei Materiali, Università di Milano-Bicocca, Via R. Cozzi, 53, 20125,
Milano, Italy

Supporting Information

Preparation of the samples

To prepare CZ05, 0.024g of $\text{Ce}(\text{OC}_3\text{H}_7)_4$ were dissolved in 5ml of $\text{C}_3\text{H}_7\text{OH}$. Then 5.4ml of $\text{Zr}(\text{OC}_3\text{H}_7)_4$ were added to the solution and finally 3ml of double distilled water were added to start hydrolysis. The sol produced by hydrolysis was aged in air until the formation of a gel which was then dried at 333K. Finally the powder was calcined at 723 K in air for 2 hours. Pure ZrO_2 and CeO_2 were prepared starting from the same precursors in analogous way.

Characterization techniques

Powder X-rays diffraction (XRD) patterns were recorded with a PANalytical PW3040/60 X'Pert PRO MPD using a copper K_α radiation source (0.15418 nm). The intensities were obtained in the 2θ ranges between 20° and 80° . The X'Pert High-Score software was used for data handling. The MAUD 2.26¹ software was used for Rietveld refinement. To determine the instrumental function the pattern obtained by a well crystallized silicon standard (crystallite size = 1 μm) was used.

The surface area measurements were carried out on a Micromeritics ASAP 2020/2010 using the Brunauer-Emmett-Teller (BET) model on the N_2 adsorption measurement. Prior to the adsorption run, all the samples were outgassed at 573K for 3 h.

The UV-Vis absorption spectra were recorded using a Varian Cary 5 spectrometer, coupled with an integration sphere for diffuse reflectance studies, using a Carywin-UV/scan software. A sample of PTFE with 100% reflectance was used as reference.

Electron Paramagnetic Resonance (EPR) spectra, recorded at room temperature and at liquid nitrogen temperature, were run on a X-band CW-EPR Bruker EMX spectrometer equipped with a cylindrical cavity operating at 100 kHz field modulation. The effect of light on EPR spectra was investigated irradiating the sample in the EPR resonant cavity by a 1000 W mercury/Xenon lamp (Oriel Instruments) equipped with a IR water filter to avoid over-heating.

The generation of radical species in solution was monitored by the EPR-spin trapping technique using a Miniscope 100 spectrometer from Magnettech and DMPO (5,5-dimethyl-1-pyrroline-N-oxide, Alexis Biochemicals, San Diego, CA) as spin trapping agent.

Computational details

Spin-polarized DFT calculations were performed using the CRYSTAL code based on a linear combination of atomic orbitals (LCAO). The hybrid B3LYP functional which gives a good estimate of the Kohn-Sham band gap has been used in all calculations. A 8-4111(d1) Gaussian-type basis set was used for the O atoms; for Zr we used a 311(d31) basis set associated with the Hay and Wadt effective core pseudopotential (ECP); for Ce we used 4321(d61)(f431) basis set associated with the Stuttgart-Dresden effective core potential. The reciprocal space is sampled using a regular sublattice with a shrinking factor of 2, and the SCF convergence was set to 10^{-6} a.u.

A 108-atoms $3 \times 3 \times 2$ supercell was generated for the calculations. Full geometry relaxation (atom locations and cell parameters) was performed with no symmetry constraint using a Broyden-Fletcher-Goldfarb-Shanno scheme. The convergence criteria was set to an RMS of the gradient of 3×10^{-4} a.u. and an RMS of the maximum atomic displacement of 1.2×10^{-3} a.u. The computed cell parameters of pure tetragonal ZrO_2 , P42/nmc space group, $a = 3.6055 \text{ \AA}$ and $c = 5.1797 \text{ \AA}$, are in reasonable agreement with previous calculations and experimental results². Each Zr atom has 4 nearest neighbour O atoms at a distance of 2.06 \AA and another 4 next-nearest neighbour O atoms at a distance of 2.40 \AA . The band-gap of ZrO_2 computed at the B3LYP level at the Γ point is about 5.8 eV . This is significantly higher than the measured bandgap of 4.2 eV using electron energy loss spectroscopy (EELS)³ but within the range measured using vacuum-ultraviolet (VUV) absorption spectroscopy ($5.78\text{-}6.62 \text{ eV}$)². The VB is dominated by the O 2p states, and the CB is dominated by the Zr 4d states.

Different concentrations and arrangements of Ce atoms substituting Zr atoms in the zirconia lattice were considered. The lowest concentration, corresponding to 1 Ce every 36 Zr ions, is 2.8%. Doping levels of 2 and 5 Ce atoms per supercell (5.5 and 13.9%, respectively) were also considered, in configurations where the Ce atoms are either clustered together or spread throughout the supercell. Systems with an extra electron added were treated by adding a uniform background charge to the supercell.

Transition energy levels were calculated using a method outlined in previous publications. The vertical or optical transition energy from a state of charge $q+1$ to a state of charge q of a general defect D can be calculated as:

$$\varepsilon(q+1/q) = E_{D,q} - E_{D,q+1} = [e_{\text{LUMO}}(N-1) + e_{\text{HOMO}}(N)]/2 \quad (1)$$

where $e_{\text{HOMO}}(N)$ is the energy of the highest occupied crystal state of the system of in charge state q , and $e_{\text{LUMO}}(N-1)$ is the energy of the lowest unoccupied crystal state of the system of charge $q+1$, with both energies referenced to the top of the VB which is set as the zero energy level.

X-Ray powder diffraction analysis

Figure S1 shows the XRD patterns obtained for pure ZrO_2 , pure CeO_2 and CZ05. While in Table S1 all parameters used in the Rietveld refinement done using the MAUD software are reported. The XRD patterns show that there is no evidence of any reflection peak typical of the CeO_2 fluoritic phase.

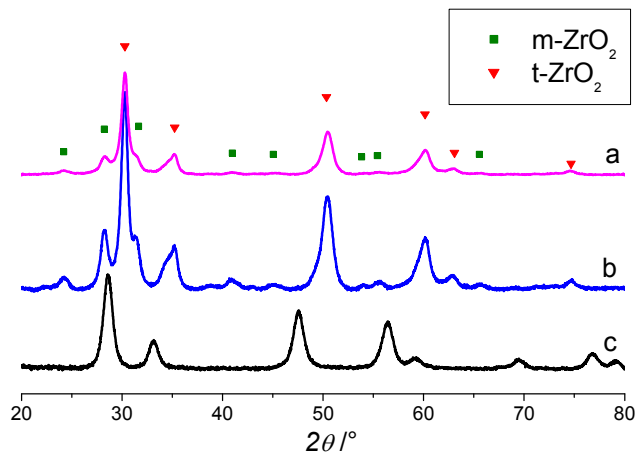


Figure S1. XRD patterns of ZrO_2 (a), CZ05 (b) and CeO_2 (c).

Table S1. Weight percentage (%wt) and lattice parameters (a, b, c, β) obtained from Rietveld refinement of the XRD patterns of bare and mixed Ce-Zr oxides. R_{wp} is the weighted residual error.

Sample	R_w	Phase	%wt	a	b	c	β
ZrO_2	4.56	t- ZrO_2	78	3.60	3.60	5.17	/
		m- ZrO_2	22	5.15	5.21	5.32	98.72
CZ05	1.45	t- ZrO_2	57	3.60	3.60	5.18	/
		m- ZrO_2	43	5.15	5.20	5.33	99.00
CeO_2	2.74	c- CeO_2	100	5.41	5.41	5.41	/

DRS characterization of mechanical mixtures

Figure S2 reports a comparison between the DR-UV-Vis spectra of two mechanical mixtures having different CeO_2 molar concentration. Increasing the CeO_2 content from 0.5% (Fig.S2b) to 10% (S2c) a band in intermediate position between the optical transitions of the two bare oxides becomes more evident.

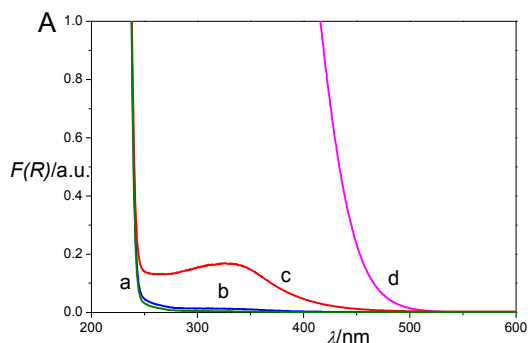


Figure S2. Absorption spectra of a) ZrO_2 , b) CZ05 mechanical mixture, c) CZ10 mechanical mixture d) CeO_2 .

EPR spectra under visible irradiation for pure ZrO₂

Figure S3 shows the EPR spectra obtained irradiating under vacuum with visible light a sample of pure ZrO₂. The experiment parallels that reported in figure 2A concerning the mixed CZ05 material and its result is markedly different. The tiny difference observed by subtracting the two spectra (Fig. S3, trace c) is actually due to the interplay between the two typical paramagnetic defects present in the pure oxide and due to Zr³⁺ and trapped electron centers⁴ (the symmetric signal at lower magnetic field) respectively. The latter center is absent in the mixed CZ05 system.

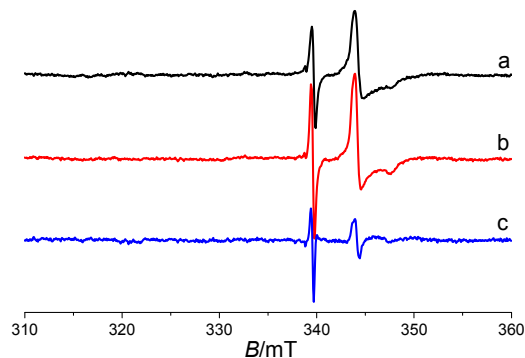


Figure S3. EPR spectra of ZrO₂ recorded at 77K under irradiation with visible light ($\lambda > 420\text{nm}$) under vacuum (a, background; b, irradiation; c, difference spectrum(b-a)).

DFT calculations: effect of Ce concentration

Substitution of more than one Zr atoms for Ce atoms was shown to cause a small broadening of the defect states, Figure S2. Clustering the Ce atoms together resulted in slightly higher dispersion of the defect states. The maximum broadening of the gap state is obtained for the case of five doping Ce atoms grouped together in the 108-atoms supercell (doping level of 13.9%, Figure S4). The total energies of the systems did not vary significantly when Ce atoms were clustered or spread out, and no special indication that the Ce dopants tend to aggregate emerges from the calculations.

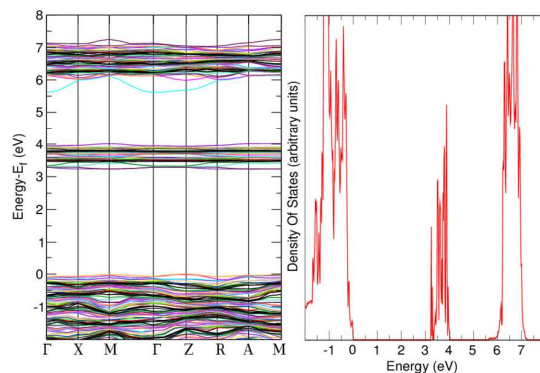


Figure S4. Band structure (left) and density of states (right) of a 3x3x2 tetragonal ZrO₂ supercell doped with 5 substitutional Ce atoms grouped together.

[¹] L. Lutterotti, *Nucl. Instrum. Methods Phys. Res. Sect. B* **2010**, 268, 334.

[²] R. H. French, S. J. Glass, F. S. Ohuchi, Y. N. Xu, W. Y. Ching, *Phys. Rev. B* **1994**, 49, 5133.

[³] D. W. McComb, *Phys. Rev. B* **1996**, 54, 7094.

[⁴] C. Gionco, M.C. Paganini, E. Giamello, R. Burgess, C. Di Valentin, G. Pacchioni, *Chem. Mater.* **2013**, 25, 2243.